

re-equilibration step with 75% A/25% B before the next injection. Flow rate was 0.7 ml min⁻¹ and the column temperature was 40 °C. The mass spectrometer (Agilent 1946D) was equipped with an electrospray ionization inlet and mass spectra were acquired in the negative ion mode. The mass spectrometer was set to selectively monitor for mass ions 294 and 296 m/z of which mass 294 m/z, the deprotonated molecular mass, was used to quantify the diclofenac residues. The mean recovery from spiked avian kidney tissue was approximately 70%, and this value was used to calculate the final sample concentration of diclofenac.

Virus isolation

Virus isolation in cell culture was performed in primary avian cell cultures prepared by the method of ref. 26 from chicken, duck and peregrine falcon embryos, and in Vero cells. Tissue samples were prepared by homogenization in Eagle's minimal essential medium with penicillin, streptomycin and amphotericin B, centrifuged to remove debris, filtered through 0.45-µm filters, and added to the cells. Cell cultures were observed daily for cytopathology. At the end of each passage (5–8 days), the cells and media were aspirated, stored at –80 °C, rapidly thawed, and added to new cells for the next passage.

Polymerase chain reaction assays for infectious agents

RNA and DNA were extracted from 0.1–0.3 g of tissue with a commercial RNA extraction kit (Trizol Reagent; BRL Life Technologies) or a commercial DNA extraction kit (Puregene; Gentra Systems) as per the manufacturer's instructions. In addition to positive and negative control RNA or DNA for each agent, intact sample RNA and DNA were verified by demonstrating the presence of avian cellular β-actin gene RNA or DNA, and the absence of nonspecific inhibitors was verified by spiking samples with positive control RNA or DNA.

The polymerase chain reaction with the reverse transcription (RT–PCR) procedure for infectious bronchitis virus was as published in ref. 27—the positive control for this assay was the Arkansas strain. The RT–PCR procedure for avian influenza was as published in ref. 28—the positive control for this assay was viral RNA obtained from the USDA National Veterinary Services Laboratory, Ames, Iowa. The RT–PCR procedure for West Nile virus was as published in ref. 29—the positive control for this assay was viral RNA obtained from the USDA National Veterinary Services Laboratory, Ames, Iowa.

Identification of *M. avium*

Acid-fast bacilli were detected with Ziehl–Neelsen stains of tissue impression smears. *Mycobacterium avium* was identified by PCR amplification and restriction enzyme polymorphisms in the heat-shock protein gene³⁰.

Uric acid measurement

Uric acid levels were measured in heparinized plasma with a colorimetric assay for the production of hydrogen peroxide by uricase.

Animal subjects

Animals were maintained and experiments performed in accordance with the Animal Health and Welfare Regulations of Bahauddin Zakariya University, Pakistan.

Received 14 September; accepted 23 December 2003; doi:10.1038/nature02317.
Published online 28 January 2004.

1. Ali, S. & Ripley, S. D. *Handbook of the Birds of India and Pakistan Together With Those of Nepal, Bhutan, and Ceylon I. Divers to Hawks* (Oxford Univ. Press, Oxford, 1968).
2. Prakash, V. Status of vultures in Keoladeo National Park, Bharatpur, Rajasthan, with special reference to population crash in *Gyps* species. *J. Bombay Nat. Hist. Soc.* **96**, 365–378 (1999).
3. Pain, D. *et al.* Causes and effects of temporospatial declines of *Gyps* vultures in Asia. *Conserv. Biol.* **17**, 661–671 (2003).
4. BirdLife International. *Threatened Birds of Asia: the BirdLife International Red Data Book* (BirdLife International, Cambridge, 2001).
5. Gilbert, M. *et al.* Breeding and mortality of Oriental White-backed vulture *Gyps bengalensis* in Punjab Province, Pakistan. *Bird Conserv. Int.* **12**, 311–326 (2002).
6. Crespo, R. & Shivaprasad, H. L. in *Diseases of Poultry* 11th edn (ed. Saif, Y. M.) 1085–1087 (Iowa State Press, Ames, 2003).
7. Beyer, W., Heinz, G. & Redmon-Norwood, A. (eds) *Environmental Contaminants in Wildlife. Interpreting Tissue Concentrations* Ch. 10, 11, 14, 17 (CRC Press, Boca Raton, 1996).
8. Swayne, D. E. & Slemmons, R. D. Comparative pathology of a chicken-origin and two-duck origin influenza virus isolates in chickens: the effect of route of inoculation. *Vet. Pathol.* **31**, 237–245 (1994).
9. Ziegler, A. F. *et al.* Nephropathogenic infectious bronchitis in Pennsylvania chickens 1997–2000. *Avian Dis.* **46**, 847–858 (2002).
10. Steele, K. E. *et al.* Pathology of fatal West Nile virus infections in native and exotic birds during the 1999 outbreak in New York City, New York. *Vet. Pathol.* **37**, 208–224 (2000).
11. Todd, P. A. & Sorkin, E. M. Diclofenac sodium. A reappraisal of its pharmacodynamic and pharmacokinetic properties, and therapeutic efficacy. *Drugs* **35**, 244–285 (1988).
12. Nys, Y. & Rzasna, J. Increase in uricemia induced by indomethacin in hens or chickens. *C. R. Séances Acad. Sci. III* **296**, 401–404 (1983).
13. Paul-Murphy, J. & Ludders, J. W. Avian analgesia. *Vet. Clin. N. Am. Exotic Anim. Prac.* **4**, 35–45 (2001).
14. Murray, M. D. & Brater, D. C. Renal toxicity of the nonsteroidal anti-inflammatory drugs. *Annu. Rev. Pharmacol. Toxicol.* **33**, 435–465 (1993).
15. Gatome, C. W. *Haematology and Blood Biochemistry in Free-Living African White-Backed Vultures *Gyps africanus* in Kenya* (MSc, Univ. London, 2002).
16. Tixier, C., Singer, H. P., Oellers, S. & Muller, S. R. Occurrence and fate of carbamazepine, clobfibrac acid, diclofenac, ibuprofen, ketoprofen, and naproxen in surface waters. *Environ. Sci. Technol.* **37**, 1061–1068 (2003).
17. Baert, K. & De Backer, P. Comparative pharmacokinetics of three non-steroidal anti-inflammatory drugs in five bird species. *Comp. Biochem. Physiol. C* **134**, 25–33 (2003).

18. Daughton, C. G. & Ternes, T. A. Pharmaceuticals and personal care products in the environment: agents of subtle change. *Environ. Health Perspect.* **107**, 907–938 (1999).
19. Henny, C. J., Blus, L. J., Kolbe, E. J. & Fitzner, R. E. Organophosphate insecticide (famphur) topically applied to cattle kills magpies and hawks. *J. Wildl. Mgmt* **49**, 648–658 (1985).
20. Langelier, K. M. in *Raptor Biomedicine* (eds Redig, P. T., Cooper, J. E., Rempfle, J. D. & Hunter, D. B.) 231–232 (Univ. Minnesota, Minneapolis, 1993).
21. McKellar, Q. A. Ecotoxicology and residues of anthelmintic compounds. *Vet. Parasitol.* **72**, 413–435 (1997).
22. Cunningham, A. A. *et al.* Indian vultures: victims of an infectious disease epidemic? *Anim. Conserv.* **6**, 189–197 (2003).
23. Mishra, S. K. *et al.* Vulture mortality: pathological and microbiological investigations. *Indian J. Anim. Sci.* **72**, 283–286 (2002).
24. Ellman, G. L., Courtney, K. D., Andres, V. & Featherstone, R. M. A new and rapid colorimetric determination of acetylcholinesterase activity. *Biochem. Pharmacol.* **7**, 88–95 (1961).
25. Hill, E. F. & Fleming, W. J. Anticholinesterase poisoning of birds: field monitoring and diagnosis of acute poisoning. *Environ. Toxicol. Chem.* **1**, 27–38 (1982).
26. Dochertry, D. E. & Slota, P. G. Use of muscovy duck embryo fibroblasts for the isolation of viruses from wild birds. *J. Tissue Cult. Methods* **11**, 165–170 (1988).
27. Kwon, H. M., Jackwood, M. W. & Gelb, J. Differentiation of infectious bronchitis virus serotypes using polymerase chain reaction and restriction fragment length polymorphism analysis. *Avian Dis.* **37**, 194–202 (1993).
28. Lee, M. S., Chang, P., Shien, J., Cheng, M. & Shieh, H. K. Identification and subtyping of avian influenza viruses by reverse transcription-PCR. *J. Virol. Methods* **97**, 13–22 (2001).
29. Johnson, D. J., Ostlund, E. N., Pedersen, D. D. & Schmitt, B. J. Detection of North American West Nile virus in animal tissue by a reverse transcription-nested polymerase chain reaction assay. *Emerg. Inf. Dis.* **7**, 739–741 (2001).
30. Mendenhall, M. K. *et al.* Detection and differentiation of *Mycobacterium avium* and *Mycobacterium genavense* by polymerase chain reaction and restriction enzyme digestion analysis. *J. Vet. Diagn. Invest.* **12**, 57–60 (2000).

Supplementary Information accompanies the paper on www.nature.com/nature.

Acknowledgements The authors thank S. Pritchard, S. Donahoe and M. Asim for technical assistance, and T. Taruscio and HEJ Laboratories (Karachi) for performing diclofenac assays. We thank V. Beasley, K. Beckman, P. Benson, T. Besser, T. Cade, K. Mealey, R. Poppenga, P. Talcott, The Ornithological Society of Pakistan, Punjab Department of Wildlife and Parks, the National Council for the Conservation of Wildlife (Islamabad), World Wildlife Fund (Pakistan), and Brigadier M. Ahmed for their cooperation. This research was conducted as part of The Peregrine Fund's Asian Vulture Crisis Project and was supported by the Gordon and Betty Moore Foundation, The Peregrine Fund, Disney Wildlife Conservation Fund, San Diego Zoological Society, and the United Nations, Ivorybill and Summit Foundations.

Authors' contributions J.L.O. coordinated the overall diagnostic work and performed microbiology; M.G., M.Z.V. and A.A.K. coordinated field biology and collected samples; R.T.W. supervised field biology; C.U.M., B.A.R. and H.L.S. performed pathology; and S.A., M.J.I.C., M.A. and A.A. collected biology data and samples.

Competing interests statement The authors declare that they have no competing financial interests.

Correspondence and requests for materials should be addressed to J.L.O. (loaks@vetmed.wsu.edu).

.....
An optimal bronchial tree may be dangerous

B. Mauroy¹, M. Filoche^{1,2}, E. R. Weibel³ & B. Sapoval^{1,2}

¹*Centre de Mathématiques et de leurs Applications, Ecole Normale Supérieure de Cachan, 94235 Cachan, France*
²*Laboratoire de Physique de la Matière Condensée, CNRS Ecole Polytechnique, 91128 Palaiseau, France*
³*Department of Anatomy, University of Bern, CH-3000 Bern, Switzerland*

The geometry and dimensions of branched structures such as blood vessels or airways are important factors in determining the efficiency of physiological processes. It has been shown that fractal trees can be space filling¹ and can ensure minimal dissipation^{2–4}. The bronchial tree of most mammalian lungs is a good example of an efficient distribution system with an approximate fractal structure^{5,6}. Here we present a study of the compatibility between physical optimization and physiological robustness in the design of the human bronchial tree. We show

that this physical optimization is critical in the sense that small variations in the geometry can induce very large variations in the net air flux. Maximum physical efficiency therefore cannot be a sufficient criterion for the physiological design of bronchial trees. Rather, the design of bronchial trees must be provided with a safety factor and the capacity for regulating airway calibre. Paradoxically, our results suggest that bronchial malfunction related to asthma is a necessary consequence of the optimized efficiency of the tree structure.

In the bronchial tree, airways branch by dichotomy with a systematic reduction of their length and diameter. In the human lung, for example, the conducting airway tree ends at about 2^{17} terminal bronchioles, each of which is followed by roughly six generations of alveolar ducts that constitute the acini⁷ and are involved in gas exchange. Considering the lower part of the bronchial tree (generations 6–16) and assuming that air flow in this duct system obeys Poiseuille law (a good approximation below the sixth generation at rest⁸), a ‘best’ structure can be deduced by minimizing the total viscous dissipation in a finite tree volume. A purely mathematical argument using Lagrange multipliers² suggests that the best tree is fractal with a fractal dimension equal to 3. In such an ideal tree, the successive airway segments are homothetic with a size ratio, h , equal to $(1/2)^{1/3} \cong 0.7937$. This is what is known as the Hess–Murray law, which was first formulated by Hess⁹ for blood vessels and then developed further by Murray¹⁰.

The effect of airway geometry on ventilation can be developed as follows. Assuming that bifurcating branches are symmetric (a reasonable assumption for the deeper part of the lung), the ratio of diameter and length between generation $p - 1$ and generation p is called h_p . Denoting R and V , respectively, as the resistance and volume of a given duct, the h -reduced duct has a Poiseuille resistance of R/h^3 , because this resistance is proportional to the duct length and inversely proportional to the fourth power of the diameter. By contrast, the volume is multiplied by a factor h^3 at each generation. After p generations, the sizes are reduced by a factor $h_1 \times h_2 \times \dots \times h_{p-1}$, such that the total resistance and volume of a tree with $N + 1$ generations (indexed 0 to N) can be written as:

$$R_N = R_0 + \sum_{p=1}^N \frac{1}{2^p} \frac{R_0}{(h_1 \times h_2 \times \dots \times h_p)^3}$$

$$V_N = V_0 + \sum_{p=1}^N 2^p (h_1 \times h_2 \times \dots \times h_p)^3 V_0$$

If Φ is the global airflow, the total pressure drop is $\Delta P_N = R_N \Phi$, and the total dissipation can be written as $\Phi \Delta P_N$. This power loss can be minimized relative to h_1, \dots, h_N on the surface defined by the constraint $V_N = \Omega$. The minimum of R_N on $V_N = \Omega$ is characterized by the existence of a Lagrange multiplier, μ , such that

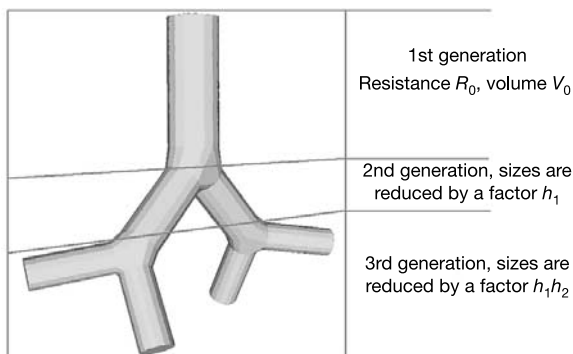


Figure 1 Geometry of a dichotomous and homothetic tree structure. In the third generation, the size reduction with respect to the first generation is the product of the homothety ratios in the second and third generations.

$\nabla(R_N) = \mu \nabla(V_N)$. The energy dissipation per unit volume of the tree, equal to $\Phi \Delta P_N / V_N$, is also optimized through this operation. This leads to $h_1 = [(\Omega - V_0)/(2NV_0)]^{1/3}$ and $h_i = (1/2)^{1/3}$ for i in the series $\{2, \dots, N\}$. The ‘best’ tree is then fractal with a constant reduction factor $h_i = (1/2)^{1/3}$. In consequence, the fractal dimension is equal to $\log(2)/\log(2^{1/3}) = 3$. For simplicity, we study here symmetric bifurcations, but, as shown below, the same results hold for asymmetric bifurcations.

More generally, assuming a constant reduction factor h between generations, the fractal dimension would be equal to $\ln(2)/\ln(1/h)$, which is larger than 3 for $h > (1/2)^{1/3}$. Figure 1 shows that with each generation the size factor falls with h , whereas the number of ducts per generation increases by a factor of 2. At generation p , therefore, the number of ducts is 2^p and the size factor is h^p . Thus, the volume and pressure drop can be written as:

$$V_N = V_0 \left[1 + \sum_{p=1}^N (2h^3)^p \right]$$

$$\Delta P_N = R_0 \Phi \left[1 + \sum_{p=1}^N \frac{1}{(2h^3)^p} \right]$$

One observes that the same factor $(2h^3)^p$ appears in both the numerator and in the denominator. Depending on whether h is smaller or larger than $(1/2)^{1/3}$, either the volume or the pressure drop is infinite for an infinitely divided tree. In other words, it is impossible to have a nonzero flux from a ‘finite’ pressure drop for an ‘infinite’ tree of finite volume. But minimizing ΔP_N for a finite tree in a given (finite) volume leads to the optimal h value equal to $(1/2)^{1/3}$.

If h is smaller than $(1/2)^{1/3} \cong 0.79$, the pressure drop for a given flux diverges with N . An increased pressure drop can be overcome by greater respiratory efforts, but in severe cases this will cause exertion. This situation can be called ‘overcritical’. In contrast, if h is larger than $(1/2)^{1/3}$, the resistance is small and the volume is larger than necessary. Notably, real lungs are not so far from optimality, with a homothety ratio h of about 0.85 (ref. 11), as shown in Fig. 2. The dependence on h of the volume and resistance of an 11-generation tree is shown in Fig. 3. Such a tree, obeying Poiseuille flow, is representative of the deeper airways in the human lung (generations 6–16). The human bronchial tree, with $h \approx 0.85$ (ref. 11), is thus not truly optimized: its volume is too large and its overall resistance is too small. This corresponds to an ‘undercritical’ condition. It gives, in fact, a safety margin for breathing with respect to possible bronchial constriction.

The fact that the homothety ratios of real bronchial trees are a few

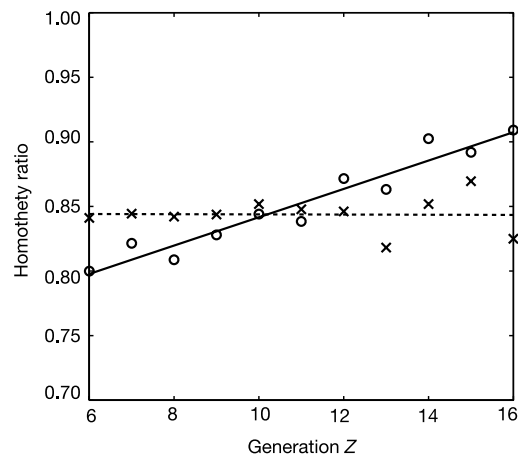


Figure 2 Homothety ratios for length and diameters of deep bronchi in the human lung ($6 \leq Z \leq 16$). Data are taken from ref. 19. Circles and crosses represent diameter and length homothety ratios, respectively.

per cent larger than the critical value has several consequences. Considered as a rigid structure, the bronchial tree would be very sensitive to geometrical imperfections. As there is always physiological variability, this would create uneven ventilation-perfusion relations in peripheral gas exchange units. This must be avoided by regulating airway calibre¹². Without such regulation, there would be a multifractal distribution of air¹³, resulting in strongly non-uniform ventilation with some regions of the lung poorly fed with fresh air. Figure 2 shows that the homothety ratio for diameter increases slightly in higher generation numbers, that is, towards the periphery. Under the hypothesis that the cast measurements reported in Fig. 2 represent the relaxed normal state of the airways, these airways allow a greater degree of contraction before a critical state is reached. In that sense, the safety margin is larger for smaller bronchioles.

In the same spirit, it should be recalled that, in asthma, bronchiolitis or allergenic reaction to pollen, the inner diameters of bronchioles, and not their lengths, are reduced. Thus, ducts are no longer homothetic and the diameter and length ratios of sequential bronchioles, denoted h_d and h_l , respectively, below, are altered. As shown in Fig. 2, the length reduction ratio h_l is constant and equal to 0.85, whereas h_d increases from 0.82 to 0.9. As the Poiseuille resistance is affected by the fourth power of the bronchial diameters, the pressure drop is:

$$\Delta P_N = R_0 \Phi \left[1 + \sum_{p=1}^N \frac{1}{2^p} \left(\frac{h_l}{h_d} \right)^p \right]$$

The fourth-power dependence of the duct resistances modifies the critical value of h_d to $(h_l/2)^{1/4} \cong 0.81$, assuming a constant value of $h_l = 0.85$.

The multiplicative effect of the tree structure combined with the fourth-power dependence of airway resistance creates an extreme sensitivity to variations in the homothety factor (see Methods). To illustrate this effect, we have computed the resistance R_{10} as a function of the h_d values when they are diminished from their normal values given in Fig. 2. The result is shown in Fig. 4. The constriction creates a marked increase in the total resistance of the tree: a 4% reduction of the homothety ratio h_d would nearly double the tree resistance, but it would increase the resistance of a simple airway tube by only 15%.

It is important to determine whether these results are applicable to the real human lung, where the bronchial tree has a marked degree of asymmetry modulating its regular features^{11,14}. Applying

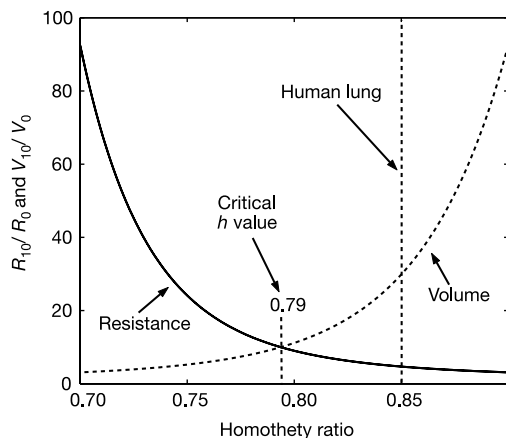


Figure 3 Dependence on the homothety ratio (h) of the resistance (R) and volume (V) of an 11-generation homothetic tree. Note the rapid variations, which indicate that the properties of the system are highly sensitive to its geometry. The homothety ratio of human airways is larger than the critical value.

the same approach, we consider an asymmetric tree built with two different reduction ratios h_1 and h_2 assigned randomly to the daughter branches at each bifurcation. Although the structure is random, the tree resistance can be written exactly as:

$$R_N = R_0 \left[1 + \sum_{p=1}^N \left(\frac{1}{h_1^3 + h_2^3} \right)^p \right]$$

The behaviour of this series is determined by the value of $1/(h_1^3 + h_2^3)$. To give an example, we have computed the effect of nonsymmetric bifurcations in which one of the branch has a systematic 20% increase in h ($h_1 = 1.2h$), whereas the other has a systematic decrease of 20% ($h_2 = 0.8h$). This corresponds to a ratio of $(1.2/0.8)^3 \cong 3.38$ between the daughter branch resistances at any bifurcation. The critical value of h is now $h = 1/(1.2^3 + 0.8^3)^{1/3} \cong 0.76$, instead of 0.79 for the symmetric model. As shown in Fig. 4, the extreme sensitivity to bronchial constriction remains (it is only slightly reduced) because the criticality depends on the basic tree structure and not on the symmetry. Notably, at criticality the asymmetric system has the same response as the symmetric tree. We conclude that other mammalian lungs that have a greater degree of asymmetry than the human lung, such as that of the dog, would behave in a similar fashion.

In summary, we have shown that the optimal system is dangerously sensitive to fluctuations or physiological variability, such that physical optimality cannot be the only criterion for the design of the bronchial tree. The morphology of the human bronchial tree is, however, close to providing maximal efficiency in assuring air distribution with minimal viscous dissipation. As the real bronchi are a little larger than optimal, they occupy a slightly larger volume than is strictly necessary. This gives the system a safety margin with respect to resistance, at the cost of an increased dead space that requires a larger tidal volume. In the human lung, the volume of the conducting airways is about 3% of the total lung volume, which is of the same order as each of the venous and arterial trees. The remaining 90% of the volume is occupied by the acini, where gas exchange takes place. The acini are themselves built by space-filling

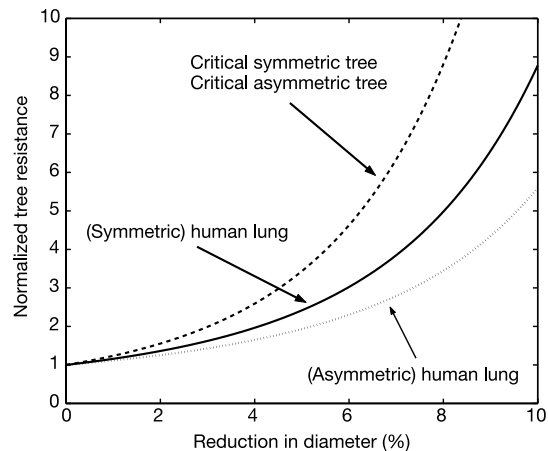


Figure 4 Dependence of tree resistance on bronchial constriction expressed as a percentage of reduction in diameter. The airway resistance has been normalized to its value without constriction. The three curves show the sensitivity of four particular trees. The dashed line corresponds to the critical trees (symmetric with $h = 0.79$ and asymmetric with $h = 0.76$). The solid line corresponds to a symmetric tree with reduction factors h_1 and h_d obtained from data for the human lung¹⁹ and shown in Fig. 2; in this system, a 4% reduction in diameter doubles the resistance. The dotted line corresponds to an asymmetric tree with an average homothety ratio of $h = 0.85$; this system is slightly less sensitive to diameter reduction, but a 5% reduction in diameter still suffices to double the resistance.

surfaces around a branched duct system, and this provides the necessary exchange surface between air and blood¹⁵.

We can draw another general conclusion from the large sensitivity of the airway system to morphology. From a strictly physical point of view, minor differences among individuals can induce considerable differences in respiratory performance. This may explain why athletes are particularly sensitive to the effects of asthma or exercise-induced bronchospasm¹⁶. The higher performance of athletes resulting from increased aerobic capacity of muscle induced by training^{7,17,18} requires higher ventilation rates to ensure an adequate oxygen supply, but this is not accompanied by a commensurate training-induced adjustment of lung structure. The higher air-flow rates must be achieved in the given bronchial tree and thus airway geometry becomes critical. An exercise-induced narrowing of small airways results in a reduction of the homothety factor h_d , which causes the flow resistance to increase steeply. This would be particularly hazardous if the homothety ratio of relaxed airways was close to its critical value of 0.79, because athletes working at their limit might not have the reserve to increase the work of breathing that this would impose. The fact that there are athletes that are capable of high performance in spite of exercise-induced bronchospasm may indicate that the homothety factor of airway branching has a sufficient safety margin to allow them adequate ventilation of their pulmonary gas exchanger. A 'more optimal' design of the airway tree would be dangerous. □

Methods

The total tree resistance can be expressed exactly as:

$$R_N = R_0 \left[1 + \sum_{p=1}^N \frac{1}{2^p} \left(\frac{h_1}{h_d} \right)^p \right] = R_0 \frac{1 - r^{N+1}}{1 - r}$$

where $r = h_1/2h_d$. The tree resistance is then a nonlinear function of $1/h_d^4$.

Received 29 July; accepted 11 December 2003; doi:10.1038/nature02287.

1. Mandelbrot, B. *The Fractal Geometry of Nature* (W. H. Freeman, San Francisco, CA, 1982).
2. West, G. B., Brown, J. H. & Enquist, B. J. A general model for the origin of allometric scaling laws in biology. *Science* **276**, 122–126 (1997).
3. Brown, J. H., West, G. B. & Enquist, B. J. *Scaling in Biology* (Oxford Univ. Press, Oxford, UK, 2000).
4. Bejan, A. *Shape and Structure, From Engineering to Nature* (Cambridge Univ. Press, Cambridge, UK, 2000).
5. Nelson, T. R. & Manchester, D. K. Modeling of lung morphogenesis using fractal geometries. *IEEE Trans. Med. Imaging* **7**, 321–327 (1988).
6. West, B. J., Barghava, V. & Goldberger, A. L. Beyond the principle of similitude: renormalization in the bronchial tree. *J. Appl. Physiol.* **60**, 1089–1097 (1986).
7. Weibel, E. R. *The Pathway for Oxygen* (Harvard Univ. Press, Cambridge, MA, 1984).
8. Mauroy, B., Filoche, M., Andrade, J. S. & Sapoval, B. Interplay between geometry and flow distribution in an airway tree. *Phys. Rev. Lett.* **90**, 1–4 (2003).
9. Hess, W. R. Das Prinzip des kleinsten Kraftverbrauchs im Dienste hämodynamischer Forschung. *Archiv Anat. Physiol.* **1914**, 1–62 (1914).
10. Murray, C. D. The physiological principle of minimum work. I. The vascular system and the cost of blood. *Proc. Natl Acad. Sci. USA* **12**, 207–214 (1926).
11. Weibel, E. R. in *The Lung: Scientific Foundations* 2nd edn Vol. 1 (eds Crystal, R. G., West, J. B., Weibel, E. R. & Barnes, P. J.) 1061–1071 (Lippincott-Raven, Philadelphia, PA, 1997).
12. Que, C. L., Kenyon, C. M., Olivenstein, R., Macklem, P. T. & Maksym, G. N. Homeokinesis and short-term variability of human airway caliber. *J. Appl. Physiol.* **91**, 1131–1141 (2001).
13. Sapoval, B. *Universalités et Fractales* (Flammarion, Paris, 1997).
14. Kitaoka, H., Ruyji, T. & Suki, B. A three-dimensional model of the human airway tree. *J. Appl. Physiol.* **87**, 2207–2217 (1999).
15. Sapoval, B., Filoche, M. & Weibel, E. R. Smaller is better—but not too small: a physical scale for the design of the mammalian pulmonary acinus. *Proc. Natl Acad. Sci. USA* **99**, 10411–10416 (2002).
16. Wilber, R. L. et al. Incidence of exercise-induced bronchospasm in Olympic winter sport athletes. *Med. Sci. Sports Exerc.* **32**, 732–737 (2000).
17. Weibel, E. R. *Symmorphosis* (Harvard Univ. Press, Cambridge, MA, 2000).
18. Hoppeler, H. & Fluck, M. Plasticity of skeletal muscle mitochondria: structure and function. *Med. Sci. Sports Exerc.* **35**, 95–104 (2003).
19. Weibel, E. R. *Morphometry of the Human Lung* (Springer, Berlin, 1963).

Acknowledgements The authors wish to thank J. M. Morel and M. Bernot for useful discussions.

Competing interests statement The authors declare that they have no competing financial interests.

Correspondence and requests for materials should be addressed to B.S. (Bernard.Sapoval@polytechnique.fr).

Susceptibility to leprosy is associated with *PARK2* and *PACRG*

Marcelo T. Mira^{1,2*}, Alexandre Alcaïs^{3*}, Nguyen Van Thuc⁴, Milton O. Moraes⁵, Celestino Di Flumeri¹, Vu Hong Thai⁴, Mai Chi Phuong⁴, Nguyen Thu Huong⁴, Nguyen Ngoc Ba⁴, Pham Xuan Khoa⁴, Euzenir N. Sarno⁵, Andrea Alter¹, Alexandre Montpetit⁶, Maria E. Moraes⁷, José R. Moraes⁷, Carole Doré⁶, Caroline J. Gallant¹, Pierre Lepage⁶, Andrei Verner⁶, Esther van de Vosse⁸, Thomas J. Hudson^{1,6}, Laurent Abel³ & Erwin Schurr¹

¹McGill Centre for the Study of Host Resistance and Departments of Human Genetics, Medicine and Biochemistry, McGill University, 1650 Cedar Avenue, Montreal, PQ H3G1A4, Canada
²Centro de Ciências Biológicas e da Saúde, Pontifícia Universidade Católica do Paraná. Rua Imaculada Conceição, 1155, CEP 80215-901, Curitiba, Paraná, Brasil
³Laboratoire de Génétique Humaine des Maladies Infectieuses, INSERM U.550, Faculté de Médecine Necker, Université de Paris René Descartes, 156 rue de Vaugirard, 75015 Paris, France
⁴Hospital for Dermato-Venereology, Nguyen Thong Street, District 3, Ho Chi Minh City, Vietnam
⁵Leprosy Laboratory, Tropical Medicine Department Oswaldo Cruz Institute, FIOCRUZ 20221-903 Rio de Janeiro, Brazil
⁶McGill University and Genome Québec Innovation Centre, 740 Docteur Penfield, Montreal, PQ H3A 1A4, Canada
⁷Laboratório de Imunogenética, Instituto Nacional do Cancer, Ministério da Saúde, 20230-130 Rio de Janeiro, RJ, Brazil
⁸Department of Infectious Diseases & Department of Immunohematology and Blood Transfusion, Leiden University Medical Center, Building 1, Albinusdreef 2, 2333 ZA Leiden, The Netherlands

* These authors contributed equally to this work

Leprosy is caused by *Mycobacterium leprae* and affects about 700,000 individuals each year¹. It has long been thought that leprosy has a strong genetic component², and recently we mapped a leprosy susceptibility locus to chromosome 6 region q25–q26 (ref. 3). Here we investigate this region further by using a systematic association scan of the chromosomal interval most likely to harbour this leprosy susceptibility locus. In 197 Vietnamese families we found a significant association between leprosy and 17 markers located in a block of approx. 80 kilobases overlapping the 5' regulatory region shared by the Parkinson's disease gene *PARK2* and the co-regulated gene *PACRG*. Possession of as few as two of the 17 risk alleles was highly predictive of leprosy. This was confirmed in a sample of 975 unrelated leprosy cases and controls from Brazil in whom the same alleles were strongly associated with leprosy. Variants in the regulatory region shared by *PARK2* and *PACRG* therefore act as common risk factors for leprosy.

The 90% confidence interval⁴ for placement of the chromosome 6q25–q26 leprosy susceptibility locus that we previously identified³ is defined by markers *D6S415* and *D6S1277*. The latter two markers are separated by 6.4 megabases (Mb) of chromosomal DNA on build 33 of the annotated human genome sequence (http://www.ncbi.nlm.nih.gov), and 31 genes with known or predicted function are located in this interval (Fig. 1a). By comparative genome sequencing and database searching, we developed a panel of 64 informative single-nucleotide polymorphisms (SNPs) (minor allele frequency more than 5%) with at least one SNP located close to or within each known gene (Fig. 1a, Supplementary Table 1). With these 64 markers, we conducted an association scan of the linkage peak interval among 197 Vietnamese families composed of two parents and one leprosy-affected child. Six markers were associated with leprosy susceptibility ($P < 0.05$), of which four, including the two most significant, were clustered in the promoter region of the *PARK2* and *PACRG* genes (Fig. 1a).